



# 4E analysis and tri-objective optimization of a triple-pressure combined cycle power plant with combustion chamber steam injection to control NO<sub>x</sub> emission

Iman Fakhari<sup>1</sup> · Parsa Behinfar<sup>1</sup> · Farhang Raymand<sup>1,2</sup> · Amirreza Azad<sup>1</sup> · Pouria Ahmadi<sup>1</sup> · Ehsan Houshfar<sup>1</sup> · Mehdi Ashjaee<sup>1</sup>

Received: 4 September 2020 / Accepted: 14 December 2020 / Published online: 25 February 2021  
© Akadémiai Kiadó, Budapest, Hungary 2021

## Abstract

This article presents a novel triple-pressure combined cycle power plant (CCPP) with a heat recovery steam generator (HRSG) configured with heat exchangers of multiple pressure levels, same as the real case. In addition, combustion chamber steam injection is added to the top cycle in order to reduce hazardous emissions. The research investigates energy, exergy, economic, and environmental aspects of the system to initiate sustainable development in said areas. A thorough parametric study is carried out to evaluate the effects of steam injection and other decision variable on emissions and system performance. Then, the total cost rate and the CO<sub>2</sub> index are minimized while maximizing the second law efficiency via a tri-objective optimization using the genetic algorithm. The outcome of the economic analysis is that the HRSG has the maximum total cost rate among all the components, namely 0.1673 \$/s. The environmental impact assessments indicate that the CO<sub>2</sub> and NO emission has considerable molar fractions of 0.035 and  $6.88 \times 10^{-4}$ , respectively. As a result of the tri-objective optimization, a 3D Pareto Frontier is presented, which pointed out the maximum attainable exergy efficiency is 50.32%, as well as the minimum total cost rates of 8.04 \$/s and CO<sub>2</sub> index of 0.34 kg/kWh. Finally, the scatter distribution of major decision variables revealed the optimum range of decision variables in which the optimum points of the Pareto Frontier are obtained. Accordingly, the scatter distribution showed that 46 kg s<sup>-1</sup> is the optimum value for steam injection flow rate in terms of efficiency, cost and emission optimization.

**Keywords** Exergy · Exergoeconomic · Combined cycle power plant · Steam injection · Soot emission · Triple-pressure HRSG · Tri-objective optimization

## List of symbols

$\dot{Q}$	Heat rate (kW)	$y$	Molar fraction
$\dot{W}$	Work rate (kW)	$T$	Temperature (K)
$\dot{m}$	Mass flow rate (kg s <sup>-1</sup> )	$X$	Number of mols
$V$	Velocity (m s <sup>-1</sup> )	$h$	Specific enthalpy (kJ kg <sup>-1</sup> )
$z$	Altitude (m)	LHV	Lower heating value (kJ kg <sup>-1</sup> )
$g$	Gravity constant (m s <sup>-2</sup> )	$E$	Energy or Exergy (kJ)
$\eta$	Efficiency (%)	ex	Specific exergy (kJ kg <sup>-1</sup> )
$\eta_2$	Isentropic efficiency (%)	$\bar{R}$	Universal gas constant (J K <sup>-1</sup> mol <sup>-1</sup> )
$K$	Equilibrium constant	$\dot{E}x_d$	Exergy destruction (kJ s <sup>-1</sup> )
		$\dot{C}$	Total cost rate (s <sup>-1</sup> )
		$\dot{Z}$	Equipment cost (s <sup>-1</sup> )
		$n$	Working hours per year
		CRF	Capital recovery factor
		$\varphi$	Maintenance factor
		$r_p$	Pressure ratio
		$\Delta T$	Temperature difference (K)
		$U$	Universal heat transfer coefficient (W m <sup>-2</sup> K <sup>-1</sup> )
		$A$	Area (m <sup>2</sup> )

✉ Pouria Ahmadi  
Pahmadi@ut.ac.ir

<sup>1</sup> School of Mechanical Engineering, College of Engineering, University of Tehran, P.O. Box 11155-4563, Tehran, Iran

<sup>2</sup> Department of Energy Engineering, School of Industrial and Information Engineering, Politecnico di Milano, 29121 Piacenza, Italy

PP	Pinch point temperature (K)
$m$	Mass (kg)
$c$	Specific heat capacity ( $\text{kJ kg}^{-1} \text{K}$ )
$\Delta T_{\text{sh}}$	Superheating temperature difference (K)
injection	Combustion chamber injected steam

### Subscripts and abbreviations

cv	Control volume
ac	Air compressor
i	Inlet
o	Outlet
$k_{\text{th}}$	For $k$ th component
f	Fuel or formation
T	At temperature T
0	At ambient condition
GT	Gas turbine
ST	Steam Turbine
w	Water
a	Air
g	Gas
HP	High pressure
IP	Intermediate pressure
LP	Low pressure
Tot	Total
env	Environment
FWP	Feedwater pump
Cond	Condenser
s	Steam
p	Pump
D	Destruction
ex	Exergy
th	Thermal
ph	Physical
ch	Chemical
cc	Combustion chamber
HRSG	Heat recovery steam generator
eco	Economizer
evp	Evaporator
lm	Logarithmic mean
LMTD	Logarithmic mean temperature difference
comb	Combustion
FP	Feed pump

## Introduction

Energy conversion is performed all around us, from cooling and heating systems to power generation systems based on nuclear energy. For decades, the ever-increasing need for electricity has been satisfied by building more steam cycle power plants, which, though improving steadily over time, still leave a lot to be desired economically as well as environmentally, which is why, optimization of energy systems,

given the limitations and environmental impacts of fossil fuels, is of great importance in the current global scene. As a result, engineers are continuously seeking new ways to raise the efficiency of older plants, reach emission standards, all while minimizing costs per generated power [1]. This can be done either by improving materials that are used in a plant, meaning they would be able to withstand higher temperatures or combining and retrofitting older plants to make a new combined cycle with advanced  $\text{CO}_2$  capture storage techniques. The former is rather slow progress since these metallurgical advancements do not happen overnight. The latter is the more practiced strategy. However, Energy engineers today face novel challenges compared with those of the past. Namely, different technology options, issue of climate change and socioeconomic conditions, all of which require delicate methods of approach and must culminate in a design that incorporates inexpensive investment and maintenance costs, flexibility in working fuels, short construction time, low environmental impact, high reliability and finally an adequate efficiency [2]. Considering the issues discussed above, it has become increasingly important to know the mechanisms responsible for the destruction of energy and resources. Moreover, having a systematic approach to design an energy conversion system and considering environmental pollutants is of great importance. Therefore, the optimization of energy systems has become of the most impactful elements of engineering [3, 4].

Traditionally, first law analysis gives us equations based on energy conservation. However, they do not grant any information about the quality and quantity of losses and do not locate the elements responsible for them. These limitations drive us to utilize exergy analysis, which is a result of the second law of thermodynamics. Exergy is commonly defined in scientific nomenclature as the maximum possible work available within any given system [5]. The term thermo-economics is the link between thermodynamics and economics, in which prices are attributed to exergy carriers and not energy carriers. Different approaches have been taken with these analyses in the past 20 years, namely average costing (AVCO), last in first out (LIFO), specific exergy costing (SPECOC), exergy costing (EXCO), thermo-functional analysis (TFA) by Lozano and Valero [6], and engineering functional analysis (EFA) by Lazzaretto and Tsatsaronis [7].

Generally, researchers have either paid attention to the upstream cycle or the downstream cycle. Very few have tried to optimize the combined cycle as a whole. If one only aims to improve the efficiency of the cycle, investment costs will rise drastically, which is why today, plant design involves increasing efficiency while keeping cost increase to a minimum. This is where thermoeconomics analysis comes into play [8]. Mohagheghi et al. [9] performed an analysis of HRSG and proceeded to optimize it using the genetic

algorithm. They also took into consideration the best performing order of different sections of the HRSG. Bracco and Silvia [10] modeled a single pressure combined cycle power plant. They optimized HRSG's pressure levels for a given gas turbine outlet temperature. They analyzed other parameters as well, such as turbine outlet steam quality, HRSG outlet temperature, and turbine blade thickness. Woudstra et al. [11] carried out a thorough analysis of a combined cycle. They considered the impact of the number of HRSG sections on efficiency. The results were that by increasing the number of sections, one decreases the exergy of outlet gas and increases efficiency and that, in general, a triple-pressure HRSG with reheater performs the best out of all models. Mansouri et al. examined how changing pressure levels of HRSG affects on-cycle and exergy efficiency. They concluded that having more pressure levels is synonymous with less exergy destruction, and higher exergy efficiency for HRSG and the whole cycle. Many authors such as Franco and Casarosa [12], Valdes and Rapun [13], and Bassily [14], [15], have worked on thermodynamic optimization, while some have worked on economic optimization, for instance, Valdes et al. [16] and Casarosa et al. [17]. Tyagi and Khan [18] investigated how temperatures in a variety of locations along the cycle impact the efficiency of overall cycle. Bassily [14] evaluated how pinch point and gas turbine inlet temperatures affect a bi-pressure CCPP's efficiency. Moreover, he came up with an optimum model to decrease cycle irreversibility and found that through optimization it is possible to increase efficiency up to 2 to 3 percent. He compared the results of the optimization against typical triple-pressure combined cycle with reheat Bassily [15]. Boonnasa et al. [19] considered the performance of a plant in Bangkok with double 110 MW GTs and a 115 MW steam turbine in standard conditions. Gas turbines were cooled by absorption chillers that would cool inlet air down to 15 °C. furthermore, it used a thermal energy storage tank to keep the heat of the cooled water to satisfy daily cooling loads. An economic and exergy analysis were performed on a 500 MW plant by Kwak et al. [20] and they were able to calculate the cost of produced electricity per kWh, considering investment and maintenance costs of equipment. Fiaschi and Giampaolo [21] focused their attention on the analyzing a semi-closed CCPP and found that combustion, HRSG, water injection and water reheater constitute the majority of losses, accounting for nearly 80 percent of all cycle losses. Cihan et al. [22] made an economic analysis of a plant in Turkey. They concluded that combustion, HRSG and GT are the main sources of losses, being responsible for about 85 percent of them. Some work has also been published on injection. Nihed et al. [23] inspected the injection of steam into the combustion chamber both from the inside and outside of the plant. They demonstrated that when injection is done from the outside, increasing the injection rate results in increase of total

efficiency. The opposite is true for injection from the inside, meaning that it decreases overall efficiency. Hamid Mokhtari et al. [24] also investigated a CCPP with steam injection. They extracted steam from low-pressure section of HRSG and found that steam injection increased power by about 2 MW, reduced costs and improved efficiency from 42 to 47 percent. Hassan Athari et al. [25] investigated a combined cycle plant running on biomass that utilized steam injection. Compressor inlet air was cooled using a FOG system, and it was observed that the cost of steam injection operation system was far lower than that of the produced power.

This paper aims to develop a method for optimization of a real triple-pressure CCPP with a new configuration of HP, IP, and LP sections considering exergoeconomic and environmental indicators. Using existing theorems on the subject, and analyzing the injection of steam to the combustion chamber, the following objectives are investigated:

- Mathematical modeling of a real Siemens triple-pressure combined cycle with a few simplifications
- Gathering the results on exergy efficiency and destruction values for each component
- Determining the part of the system with the highest exergy destruction
- Solving the combustion with detailed soot emissions ( $\text{NO}_x$  and CO) using equilibrium constants
- Investigating the effect of steam injection on efficiency, total cost rate and emissions
- Cost, efficiency and emission multi-objective optimization
- Presenting a 3D Pareto Frontier as a result of the genetic algorithm multi-objective optimization
- Illustrating scatter distributions to determine optimum value for decision variables

## Cycle description and assumptions

A combined cycle PP is comprised of a Bryton cycle upstream and a Rankine cycle downstream (Fig. 1). First, air with ambient properties is fed into the compressor where its pressure and temperature are increased (state 1,2). Then, the air is mixed with fuel and the mixture enters the combustion chamber, and the combustion process happens with a steam injection to avoid soot emissions production (state 3). Flue gases are directed to the gas turbine, causing it to generate power (state 4). After expansion, these gasses enter the triple-pressure HRSG to heat an opposing water stream in order to generate steam. The proposed CCPPs have two gas turbines connected to one HRSG because the investment cost of an HRSG is too high, and this type of connection reduces a substantial amount of power plant capital cost. Thus, the joint exhaust at state 4 firstly enters the reheat and

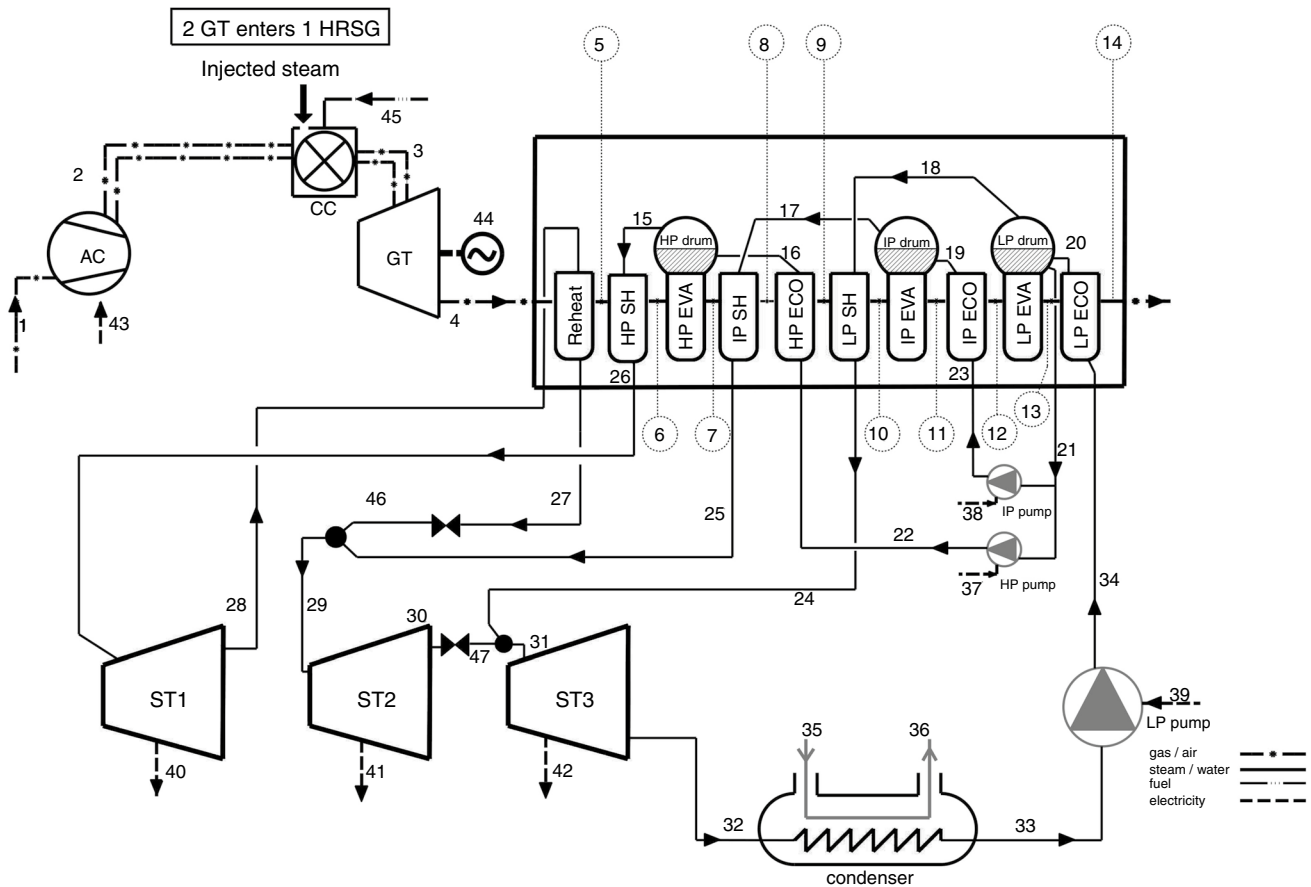


**Fig. 1** Schematic view of the proposed triple-pressure combined cycle power plant with steam injection

HRSG HP section. In the HP section, the required steam for the HP steam turbine power plant produced (state 26), and the outlet stream of the turbine enters the reheater, which generates a portion of the IP steam turbine inlet steam utilizing a pressure regulator (state 26, 46). The next section is the IP section, which produces superheated steam (state 25) and mixed with the mentioned stream of the reheater and enters the IP steam turbine (state 29). The outlet stream of the IP steam turbine is still a saturated vapor that has the potential to be used again. Utilizing a pressure regulator (state 30, 47), the saturated vapor mixed (state 31) with the superheated steam comes from the LP section (state 24) and enters the LP steam turbine. Finally, the out-stream of the LP steam turbines passes through a condenser (state 32) to be condensed and be ready to be pumped (state 33). As mentioned in the introduction section, this special configuration of HRSG is a simulation of Siemens's new generation triple-pressure HRSG, which recovers the highest possible amount of heat from the upstream exhaust.

All of the formulas presented so far would have to be solved with relevant constraints, in order to yield proper results. These constraints are:

- There is a maximum value for amount of steam injected into combustion chamber; this value is derived as a function of relative humidity and pressure of dew point.
- The pressure drops in the HRSG is negligible.
- Gas turbine and steam turbine inlet temperatures have to be lower than a maximum value, here taken to be 1500 and 900 K, respectively (availability constraints).
- HRSG outlet temperature must be lower than acidic dew point.
- The pressure drop in the condenser is negligible.

## Methodology

A group of parameters is taken to be the input values according to the previous researches [15]. These include compressor and turbine pressure ratios, air mass flow rate, fuel flow rate which is derived according to fuel-to-air ratio (normally the molar ratio of fuel-to-air is 0.03), condenser pressure,

steam turbine pressures, pinch point temperature of each section of HRSG, isentropic efficiency of all pumps, turbines and compressor as well as pressure drop in combustion chamber (assumed 2%), heat losses from combustion chamber, injected steam mass flow rate and amount of super heating in each super heater.

**Energy analysis**

Energy analysis is a direct result of the first law of thermodynamics, likewise known as “conservation of energy.” The majority of systems we deal with are open systems, meaning that streams of mass can enter and exit from the system. This is true for power and cooling systems. For an open system, we have the below equation from thermodynamics:

$$\left(\frac{dE}{dt}\right)_{CV} = \dot{Q} - \dot{W} + \sum \dot{m}_i \left( h_i + \frac{V_i^2}{2} + gz_i \right) - \sum \dot{m}_o \left( h_o + \frac{V_o^2}{2} + gz_o \right) \tag{1}$$

In the following subsection, we rewrite energy equations for each part of the cycle.

**Compressor**

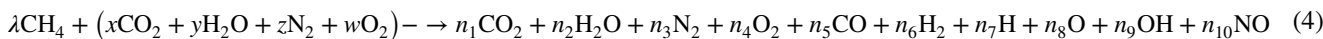
Initially, the air is brought into the compressor at ambient conditions and is compressed up to point 2. Main equations for the compressor are:

$$\dot{W}_{ac} = \dot{m}_a (h_2 - h_1) \tag{2}$$

$$\eta_{2ac} = \frac{h_{2s} - h_1}{h_2 - h_1} \tag{3}$$

**Combustion chamber**

The main relation in combustion chamber is based on the chemical equation, which is given below:



In this equation, there are 11 unknowns (product temperature and  $n_1$  to  $n_{10}$ ) with 11 equations. The first four relations can be written for atomic balancing of C, H, O, and N. Then, another six required equations are derived from equilibrium relations that are presented below, and the final equation is the energy balance of the reactants and products. It should be noted that coefficients  $x$ ,  $y$ ,  $w$ ,  $z$ , and  $\lambda$  are given as 0.0003, 0.2059, 0.7748, 0.019, and 0.035, respectively. Equilibrium relations have been taken from [26]:

$$\frac{1}{2}H_2 \leftrightarrow H, K_1 = \frac{y_7 P^{\frac{1}{2}}}{y_6^{\frac{1}{2}}} \tag{5}$$

$$\frac{1}{2}O_2 \leftrightarrow O, K_2 = \frac{y_8 P^{\frac{1}{2}}}{y_4^{\frac{1}{2}}} \tag{6}$$

$$\frac{1}{2}O_2 + \frac{1}{2}H_2 \leftrightarrow OH, K_3 = \frac{y_9}{y_4^{\frac{1}{2}} y_6^{\frac{1}{2}}} \tag{7}$$

$$\frac{1}{2}O_2 + \frac{1}{2}N_2 \leftrightarrow NO, K_4 = \frac{y_{10}}{y_4^{\frac{1}{2}} y_3^{\frac{1}{2}}} \tag{8}$$

$$\frac{1}{2}O_2 + H_2 \leftrightarrow H_2O, K_5 = \frac{y_2}{y_4^{\frac{1}{2}} y_6 P^{\frac{1}{2}}} \tag{9}$$

$$\frac{1}{2}O_2 + CO \leftrightarrow CO_2, K_6 = \frac{y_1}{y_4^{\frac{1}{2}} y_3 P^{\frac{1}{2}}} \tag{10}$$

where  $y_i$  is the molar fraction of each species and can be obtained from:

$$y_i = \frac{n_i}{\sum_{k=1}^{10} n_k} \tag{11}$$

Moreover,  $K_i$  is the corresponding equilibrium constant of each equation and can be found from polynomial coefficients which are presented below:

$$\log_{10} K_i(T) = A_i \ln \left( \frac{T}{1000} \right) + \frac{B_i}{T} + C_i + D_i T + E_i T^2 \tag{12}$$

**Table 1** Value of coefficients required for calculation of equilibrium constants in Eq. 12

$i$	Equilibrium Reaction	$A_i$	$B_i$	$C_i$	$D_i$	$E_i$
1	$\frac{1}{2}H_2 \leftrightarrow H$	+0.4321E+00	-0.1124E+05	+0.2672E+01	-0.7457E-04	+0.2424E-08
2	$\frac{1}{2}O_2 \leftrightarrow O$	+0.3108E+00	-0.1295E+05	+0.3217E+01	-0.7383E-04	+0.3446E-08
3	$\frac{1}{2}O_2 + \frac{1}{2}H_2 \leftrightarrow OH$	-0.1417E+00	-0.2133E+04	+0.8534E+00	+0.3550E-04	-0.3102E-08
4	$\frac{1}{2}O_2 + \frac{1}{2}N_2 \leftrightarrow NO$	+0.1508E-01	-0.4709E+04	+0.6460E+00	+0.2728E-05	-0.1544E-08
5	$\frac{1}{2}O_2 + H_2 \leftrightarrow H_2O$	-0.7523E+00	+0.1242E+05	-0.2602E+01	+0.2595E-03	-0.1626E-07
6	$\frac{1}{2}O_2 + CO \leftrightarrow CO_2$	-0.4153E-02	+0.1486E+05	-0.4757E+01	+0.1246E-03	-0.9002E-08

where  $A_i$ ,  $B_i$ ,  $C_i$ ,  $D_i$ , and  $E_i$  are the coefficients of the logarithmic equilibrium constant equation and is given in Table 1 [26].

**Gas Turbine**

High-temperature flue gases from combustion chamber reach the GT to make work, following the two main corresponding equations brought here:

$$\dot{W}_{GT} = \dot{m}_g (h_3 - h_4) \tag{13}$$

$$\eta_{2GT} = \frac{h_3 - h_4}{h_3 - h_{4s}} \tag{14}$$

Flue gases exiting the gas turbine are still very hot and able to produce work, which is why they are taken through the HRSG.

**Triple-pressure HRSG**

The HRSG includes three sections, economizer, evaporator and superheater, all of which are necessarily a heat exchanger where gases from gas turbine outlet are in one set of pipes and the other set of pipes houses steam with variable flow rates, according to which section it represents. General equations for these sections are written as:

$$\dot{m}_g (h_{g \text{ in}} - h_{g \text{ out}}) = \dot{m}_w (h_{w \text{ out}} - h_{w \text{ in}}) \tag{15}$$

The full set of HRSG equations and equations relating pinch point temperature values account to 18 equations that need to be solved simultaneously.

To illustrate the temperature of the exhaust and water streams in the triple-pressure HRSG, a T-Q diagram of the HRSG presented in Fig. 2 in which the pinch point temperature of LP, IP and HP sections are shown. Note that the pink line is for reheat section.

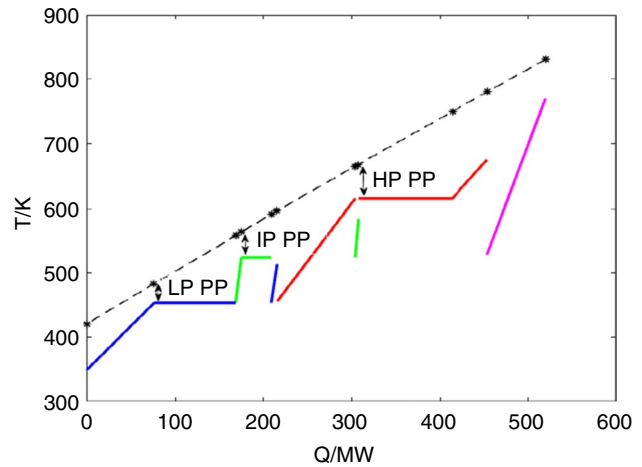


**Fig. 2** T-Q diagram of triple-pressure HRSG steam and exhaust streams

**Steam Turbine**

There are three steam turbines, all converting energy of vapor stream exiting the HRSG into work:

$$\eta_{2ST1} = \frac{h_{28} - h_{26}}{h_{28s} - h_{26}}, \dot{W}_{ST1} = \dot{m}_{HP} (h_{26} - h_{28}) \tag{16}$$

$$\eta_{2ST2} = \frac{h_{30} - h_{29}}{h_{30s} - h_{29}}, \dot{W}_{ST2} = \dot{m}_{IP} (h_{23} - h_{21}) \tag{17}$$

$$\eta_{2ST3} = \frac{h_{32} - h_{31}}{h_{32s} - h_{31}}, \dot{W}_{ST3} = \dot{m}_{LP} (h_{34} - h_{33}) \tag{18}$$

**Pumps**

Regardless of location, pumps have the responsibility of sub-cooling liquids with a quality of zero. Pumps are used in our plant to circulate extracts entering high pressure and medium

pressure economizer, as well as one pump for subcooling condenser outlet stream. The formulation for pumps is:

$$\eta_{2FWP} = \frac{h_{os} - h_i}{h_o - h_i}, \dot{W}_{FWP} = \dot{m}_p (h_o - h_i) \tag{19}$$

**Condenser**

Condenser uses seawater for the hot stream cooling, and the mass flow rate of seawater should be found around 80 times that of steam. The temperature rise of seawater is taken to be 10 K.

$$\dot{m}_s (h_{32} - h_{33}) = \dot{m}_{cond} (h_{36} - h_{35}) \tag{20}$$

**Energy Efficiency**

One can write efficiencies for the upstream, downstream, and the whole cycles as follows:

$$\eta_{GT} = \frac{\dot{W}_{GT} - \dot{W}_{AC}}{\dot{m}_f LHV} \tag{21}$$

$$\eta_{ST} = \frac{\dot{W}_{ST} - \dot{W}_{Pump}}{\dot{Q}_{HRSG}} \tag{22}$$

$$\eta_{net} = \frac{\dot{W}_{ST} - \dot{W}_{Pump} + \dot{W}_{GT} - \dot{W}_{AC}}{\dot{m}_f LHV} \tag{23}$$

**Exergy analysis**

Exergy is defined as the maximum amount of work that a system can produce if it reaches ambient, or dead state, conditions, having gone through an equilibrated process. Exergy of each system depends on the system itself and its ambient conditions. In exergy analysis, the second law of thermodynamics is used jointly with conservation of mass and energy. It enables us to locate and identify the losses and optimize the system to minimize such losses. Exergy of a system is comprised of kinetic, potential, chemical, physical, heat, and work exergy terms, all of which constitute the exergy balance for a control volume as below:

$$\left(\frac{dE}{dt}\right)_{cv} = \sum \left(1 - \frac{T_0}{T_j}\right) \dot{Q}_j - \dot{W}_{cv} + \sum \dot{m}_i e_i - \sum \dot{m}_o e_o - \dot{E}_D \tag{24}$$

A value that is of high interest in above equation is exergy destruction ( $\dot{E}_D$ ), because it represents the lost potential of a component or the whole system to produce useful work.

Accordingly, the exergy balance equation for all parts is written following the general convention seen below:

$$\dot{E}x_{in} + \dot{E}x_{fuel} = \dot{E}x_{out} + \dot{E}x_{dest} \tag{25}$$

The value of exergy for each of the streams is derived from the sum of physical and economical exergy, formulas for which are shown:

$$ex_{ph} = (h - h_0) - T_0 (s - s_0) \tag{26}$$

$$ex_{ch} = \sum X_i ex_{ch}^{0,i} + \bar{R}T_0 \sum X_i \ln(x_i) \tag{27}$$

$$ex = ex_{ch} + ex_{ph} \tag{28}$$

The exergy destruction and exergy efficiency of all components presented in Table 2. In addition, the exergy destruction for the overall HRSG can be written as:

$$Exd_{HRSG} = Ex_4 - Ex_{14} + Ex_{34} + Ex_{28} - (Ex_{27} + Ex_{25} + Ex_{24} + Ex_{26}) + W_{P1} + W_{P2} \tag{29}$$

And also, the exergy efficiency of HRSG:

$$\eta_{HRSG}^{ex} = \frac{Ex_{27} + Ex_{25} + Ex_{24} + Ex_{26} - (Ex_{34} + Ex_{28}) - (W_{P1} + W_{P2})}{Ex_4 - Ex_{14}} \tag{30}$$

**Table 2** Exergy efficiency and exergy destruction of each component

Component	Exergy Destruction	Exergy Efficiency
Condenser	$\dot{E}x_{35} + \dot{E}x_{32} - (\dot{E}x_{33} + \dot{E}x_{36})$	$\frac{(\dot{E}x_{35} - \dot{E}x_{36})}{(\dot{E}x_{33} - \dot{E}x_{32})}$
Compressor	$\dot{E}x_1 + \dot{W}_{AC} - (\dot{E}x_2)$	$\frac{(\dot{E}x_2 - \dot{E}x_1)}{\dot{W}_{AC}}$
Gas turbine	$\dot{E}x_3 - \dot{W}_{GT} - (\dot{E}x_4)$	$\frac{(\dot{W}_{GT})}{(\dot{E}x_3 - \dot{E}x_4)}$
Combustion chamber	$\dot{E}x_{in} + \dot{E}x_2 - (\dot{E}x_3)$	$\frac{(\dot{E}x_3 - \dot{E}x_2)}{\dot{E}x_{in}}$
Pump 1	$\dot{m}_{HP} ex_{21} + \dot{W}_{P1} - \dot{m}_{HP} ex_{22}$	$\frac{\dot{m}_{HP}(ex_{22} - ex_{21})}{\dot{W}_{P1}}$
Pump 2	$\dot{m}_{IP} ex_{21} + \dot{W}_{P2} - \dot{m}_{IP} ex_{23}$	$\frac{\dot{m}_{IP}(ex_{23} - ex_{21})}{\dot{W}_{P2}}$
Pump 3	$\dot{E}x_{33} + \dot{W}_{P3} - \dot{E}x_{34}$	$\frac{(\dot{E}x_{34} - \dot{E}x_{33})}{\dot{W}_{P3}}$
Turbine 1	$\dot{E}x_{26} - \dot{E}x_{28} - \dot{W}_{ST1}$	$\frac{(\dot{W}_{ST1})}{(\dot{E}x_{26} - \dot{E}x_{28})}$
Turbine 2	$\dot{E}x_{29} - \dot{E}x_{30} - \dot{W}_{ST2}$	$\frac{(\dot{W}_{ST2})}{(\dot{E}x_{29} - \dot{E}x_{30})}$
Turbine 3	$\dot{E}x_{31} - \dot{E}x_{32} - \dot{W}_{ST3}$	$\frac{(\dot{W}_{ST3})}{(\dot{E}x_{31} - \dot{E}x_{32})}$

### Economic analysis

In order to write economic balance equations for each piece of equipment in the plant, we must first know the prices for each of them. These relations are derived from [27]. The cost lost in each component is also known as the cost of exergy destruction which could be the target of a minimization analysis. The cost of exergy destruction can be found using economic balances, utilizing each component capital cost and the inlet and outlet exergies and price per exergy. The general form of cost balance can be written like below:

$$\dot{C}_{in} + \dot{Z}_k = \dot{C}_{out} \tag{31}$$

where  $\dot{Z}_k$  cost rate of each component and can be found using the purchase equipment cost or the investment cost of each component, which is presented in Table 3.

Using these values for every component, the cost rate ( $\dot{Z}$ ) can be found easily using the below equation in which CRF is the capital recovery factor [30],  $\phi$  the maintenance factor and N is the amount working hours per year in which our plant designed to operate:

$$\dot{Z}_k = \frac{Z_k(CRF)\phi}{3600N} \tag{32}$$

Finally, using these values, all the exergoeconomic balances are written and illustrated in Table 4. It can be mentioned that there are some auxiliary equations (Fuel Rule) in order to attain the proper number of equations which are presented in the corresponding components.

The cost of fuel for all components will be found by solving cost balances. Then, cost of exergy destruction can be found by:

$$\dot{C}_D = \sum c_{F,k} Ex_{dest,k} \tag{33}$$

where  $Ex_{dest,k}$  is the exergy destruction of component k and  $c_{F,k}$  is the cost of fuel for the component [27]. In addition, there is a definition for the utilized natural gas cost as fuel cost, which is:

$$\dot{C}_f = 1.06(3 \times 10^{-9}) \dot{m}_f LHV \tag{34}$$

Furthermore, finally, the environmental impact has a corresponding cost for governments as a side effect which estimated as:

$$\dot{C}_{env} = 0.024 \dot{m}_{CO_2} + 0.02086 \dot{m}_{CO} + 6.853 \dot{m}_{NO_x} \tag{35}$$

**Table 3** Purchase equipment cost formulation for all components [28, 29]

Component	Formulation	Constants
Air Compressor	$Z_{AC} = \left( \frac{c_{11} \dot{m}_{air}}{c_{12} - \eta_{AC}} \right) \left( \frac{P_2}{P_1} \right) \ln \frac{P_2}{P_1}$	$c_{11} = 44.1 \frac{\$}{kg/s}$ $c_{12} = 0.95$
Combustion Chamber	$Z_{CC} = \left( \frac{c_{21} \dot{m}_{air}}{c_{22} - \frac{P_3}{P_2}} \right) [1 + \exp(c_{23} T_3 - c_{24})]$	$c_{21} = 46.08 \frac{\$}{kg/s}$ $c_{22} = 0.995$ $c_{23} = 0.018 K^{-1}$ $c_{24} = 26.4$
Gas Turbine	$Z_{GT} = \left( \frac{c_{31} \dot{m}_{air}}{c_{32} - \eta_{GT}} \right) \left( \ln \frac{P_3}{P_4} \right) [1 + \exp(c_{33} T_3 - c_{34})]$	$c_{31} = 479.34 \frac{\$}{kg/s}$ $c_{32} = 0.94$ $c_{33} = 0.036 K^{-1}$ $c_{34} = 54.4$
HRSG		$c_{51} = 6570 \frac{\$}{(kW/K)^{0.8}}$ $c_{52} = 21276 \frac{\$}{kg/s}$ $c_{53} = 1184.4 \frac{\$}{(kg/s)^{1.2}}$
Condenser	$Z_{HRSG} = c_{51} \left[ \left( \frac{\dot{Q}_{eco}}{\Delta T_{lm,eco}} \right)^{0.8} + \left( \frac{\dot{Q}_{evp}}{\Delta T_{lm,evp}} \right)^{0.8} \right] + c_{52} \dot{m}_{st} + c_{53} \dot{m}_g^{1.2}$ $Z_{cond} = c_{61} \frac{\dot{Q}_{cond}}{k \Delta T_{lm}} + c_{62} \dot{m}_{CW} + 70.5 \dot{Q}_{cond} [-0.69 \ln(\bar{T}_{CW} - T_{WB}) + 2.1898]$	$c_{61} = 280.74 \frac{\$}{m^2}$ $c_{62} = 746 \frac{\$}{kg/s}$ $k = 2200 Wm^2 K^{-1}$
Fit pump	$Z_{FP} = c_{71} (\dot{W}_{FP})^{0.71} \left( 1 + \frac{0.2}{1 - \eta_{FP}} \right)$	$c_{71} = 705.18 \frac{\$}{kg/s}$
Steam Turbine	$Z_{ST} = c_{81} (\dot{W}_{ST})^{0.7} \left[ 1 + \left( \frac{0.05}{1 - \eta_{ST}} \right)^3 \right] \left[ 1 + 5 \exp\left( \frac{T_8 - 866}{10.42} \right) \right]$	$c_{81} = 3880 \frac{\$}{KW^{0.7}}$



**Table 4** Exergoeconomic equations (cost balances) for each component

Component	Cost balances
Air Compressor	$c_1 = 0$ $c_1 Ex_1 + c_{43} W_{AC} + Z_{AC} = c_2 Ex_2$
Combustion Chamber	$C_2 + c_{45} Ex_{in} + Z_{CC} = C_3$ $c_{45} = 3 \times 10^{-9}$
Gas Turbine	$C_3 + Z_{GT} = c_{44} W_{GT} + C_4$ Fuel rule: $c_3 = c_4$ Same power worth: $c_{43} = c_{44}$
HRSG (HP)	$C_4 + C_{28} + C_8 + C_{22} + Z_{HP} = C_{27} + C_{26} + C_7 + C_9$ Fuel Rule: $c_4 = c_8$ Fuel Rule: $c_7 = c_4$ Fuel Rule: $c_{14} = c_4$
HRSG (IP)	$C_7 + C_{10} + C_{23} + Z_{IP} = C_{25} + C_8 + C_{12}$ Fuel Rule: $c_9 = c_8$ Fuel Rule: $c_{10} = c_8$ Same Power worth for GT & ST: $c_{40} = c_{43}$
HRSG (LP)	$C_{34} + C_{12} + C_9 + Z_{LP} = C_{14} + C_{24} + C_{10} + C_{21}$
Steam Turbine 1	$C_{26} + Z_{ST1} = C_{40} W_{ST1} + C_{28}, c_{28} = c_{26}$
Steam Turbine 2	$C_{29} + Z_{ST2} = C_{41} W_{ST2} + C_{30}, c_{29} = c_{30}$
Steam Turbine 3	$C_{31} + Z_{ST3} = C_{42} W_{ST3} + C_{32}, c_{31} = c_{32}$
Condenser	$C_{32} + Z_{Cond} + C_{35} = C_{36} + C_{33}, c_{32} = c_{33}$
Contact point1	$C_{29} = C_{46} + C_{25}$
Contact point2	$C_{31} = C_{47} + C_{24}$
LP Pump	$C_{33} + c_{39} W_{Pump3} + Z_{LP} = C_{34}, c_{39} = c_{40}$
IP Pump	$C_{21} + c_{38} W_{Pump2} + Z_{IP} = C_{23}, c_{38} = c_{40}$
HP Pump	$C_{21} + c_{37} W_{Pump1} + Z_{HP} = C_{22}, c_{37} = c_{40}$
Valve 1	$C_{27} = C_{46}$
Valve 2	$C_{30} = C_{47}$

**Optimization**

Before optimizing the cycle, the objective functions must be determined. These functions include exergy efficiency, which is calculated as follows:

$$\eta_{ex} = \frac{\eta_{th}}{1.06} \tag{36}$$

In this, Eq. 1.06 corresponds to natural gas chemical exergy coefficient [31]. Also, the total cost rate of the system:

$$\dot{C}_{tot} = \sum \dot{Z}_k + \dot{C}_D + \dot{C}_{env} + \dot{C}_f \tag{37}$$

And the CO<sub>2</sub> index of the power plant:

$$\varepsilon_{CO_2} = \frac{\dot{m}_{CO_2}}{\dot{W}_{net}} \tag{38}$$

Accordingly, utilizing the genetic algorithm toolbox of MATLAB software, a multi-objective optimization is done

**Table 5** Upper and lower bounds of decision variables

Parameter	Lower bound	Upper bound
$\lambda$	0.02	0.04
Injection/kg s <sup>-1</sup>	0	50
$\eta_{GT}$	0.8	0.9
$\eta_{AC}$	0.8	0.9
$rp$	8	20
$\eta_{ST}$	0.8	0.9
$PP_{HP}/K$	30	80
$PP_{IP}/K$	10	50
$PP_{LP}/K$	10	50
HP/bar	90	180
IP/bar	15	50
LP/bar	3	12
$P_{cond}$ /kPa	10	80

with the aim of maximizing exergy efficiency while minimizing total cost rate and CO<sub>2</sub> index. The decision variables with their upper and lower bounds are presented in Table 5. These constraints are made because of availability or metallurgical limitations [15, 32, 33].

Table 6 shows the input values used for the mathematical model.

**Table 6** Proposed model input values

Parameter	Value
10	Injection /kg s <sup>-1</sup>
500	Air /kg s <sup>-1</sup>
0.035	$\lambda$
0.85	$\eta_{GT}$
0.88	$\eta_{AC}$
15	$rp$
0.9	$\eta_{ST1}$
0.9	$\eta_{ST2}$
0.9	$\eta_{ST3}$
0.88	$\eta_{P1}$
0.88	$\eta_{P2}$
0.88	$\eta_{P3}$
50	$PP_{HP}/K$
40	$PP_{IP}/K$
30	$PP_{LP}/K$
60	$\Delta Tsh_{HP}/K$
60	$\Delta Tsh_{IP}/K$
60	$\Delta Tsh_{LP}/K$
150	HP/bar
40	IP/bar
10	LP/bar
40	$P_{cond}$ /kPa
101.325	$P_0$ /kPa
298	$T_0$ /K

**Table 7** Validation of combustion composition against Ferguson et al. [34] data

Composition	Molar Fraction					
	T = 1000 K $\lambda = 0.04$			T = 1500 K $\lambda = 0.04$		
	Present Study	Ferguson et al. [34]	Abs Error/%	Present Study	Ferguson et al. [34]	Abs Error/%
CO <sub>2</sub>	0.0086	0.0083	3.61	0.0085	0.0083	2.41
H <sub>2</sub> O	0.0162	0.0166	2.41	0.0162	0.0166	2.41
N <sub>2</sub>	0.7765	0.7837	0.92	0.7759	0.7827	0.87
O <sub>2</sub>	0.1986	0.1913	3.82	0.1979	0.1909	3.67
CO	$3.16 \times 10^{-13}$	$2.97 \times 10^{-13}$	6.39	$2.54 \times 10^{-8}$	$2.39 \times 10^{-8}$	6.27
H <sub>2</sub>	$8.68 \times 10^{-13}$	$8.59 \times 10^{-13}$	1.05	$1.89 \times 10^{-8}$	$1.86 \times 10^{-8}$	1.61
H	$5.35 \times 10^{-16}$	$5.44 \times 10^{-16}$	1.65	$6.13 \times 10^{-10}$	$6.22 \times 10^{-10}$	1.45
O	$1.71 \times 10^{-11}$	$1.78 \times 10^{-11}$	3.44	$4.51 \times 10^{-7}$	$4.57 \times 10^{-7}$	1.31
OH	$2.37 \times 10^{-8}$	$2.30 \times 10^{-8}$	3.44	$1.66 \times 10^{-5}$	$1.57 \times 10^{-5}$	5.88
NO	$3.40 \times 10^{-5}$	$3.36 \times 10^{-5}$	1.32	0.0013	0.0012	8.33

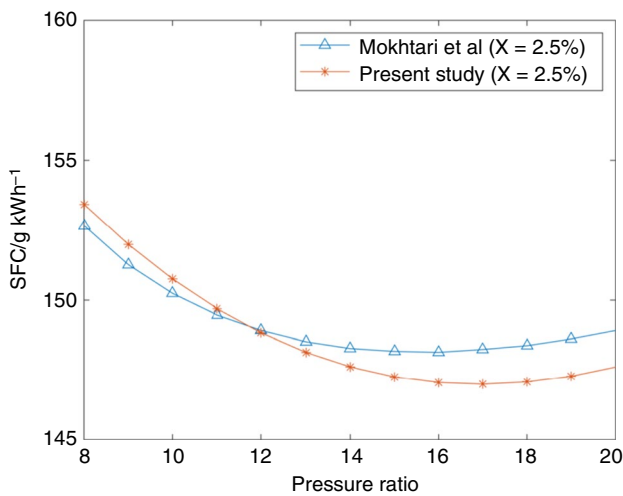


**Fig. 3** Validation of pressure ratio effect on SFC for 2.5% steam injection

### Results and discussion

In the results section, firstly, the validation of the mathematical model is presented. In the next part, the results of energy, exergy, economic and environmental assessments are presented; then, the effect of major decision variables on the performance parameters of the system is investigated in the parametric study section. Finally, a comprehensive result of tri-objective optimization, including 3D Pareto Frontier and scatter distribution of each parameter, is presented in order to demonstrate the optimum range of each decision variable.

**Table 8** Validation of gas turbine cycle against Ameri et al. [35] results for no steam injection case

Gas Turbine Cycle Components	Exergy Destruction Rate (MW)	
	Present Study at $m_{air} = 490 \text{ kg s}^{-1}$	Ameri et al. [35]
Compressor	6.12	5.99
Gas Turbine	21.21	21.01
Combustion Chamber	144.24	142.51

**Table 9** Results of exergy efficiency, purchase cost rate, and exergy destruction for all components

Component	$\eta_{ex}()$	$\dot{Z} / \frac{\$}{s}$	$Ex_{dest} / \text{MW}$
Condenser	11.23	0.1340	51.26
Compressor	94.55	0.0721	10.86
Gas Turbine	94.81	0.0433	24.53
Combustion Chamber	68.80	0.0122	165.13
Steam Turbine 1	72.53	0.0236	6.90
Steam Turbine 2	94.48	0.0453	2.69
Steam Turbine 3	69.48	0.0535	35.18
HRSG	84.30	0.1673	41.59
Total	–	0.5513	338.14

### Validation

In this section, the validation of gas turbine cycle, equilibrium combustion and also steam injection is presented. Table 7 shows the result of combustion composition validation against Ferguson et al. [34] which shows acceptable error. Figure 3 shows the validation of pressure ratio

effect on special fuel consumption (SFC) against result of Mokhtari et al. [24] study for a case with 2.5% steam injection. Table 8 illustrates the validation of gas turbine cycle against data of Ameri et al. [35] study for no steam injection case and also air mass flow rate of 490 kg s<sup>-1</sup>.

Table 9 shows the results of exergy and economic analysis. Accordingly, exergy efficiency, purchase cost rate, and the exergy destruction in every component listed. The results show that the condenser has a minimum exergy efficiency of 11.23% due to the low operating temperature and the heated waste during the condensing process. Besides, the combustion chamber has a maximum 165.13 MW exergy destruction since the combustion process instinctively destroys the exergy. Besides, the HRSG has a maximum purchase cost rate of 0.1673. Finally, the amount of environmental cost introduced in Eq. 35 found 6.24 \$/s. The value is a substantial cost rate since fixing the health impacts of hazardous emissions on humans and nature costs too much for governments.

Table 10 shows the result of environmental assessments. Accordingly, the combustion products molar fraction reported for all species. Since the temperature of the combustion is around 1500 K, most of the calculated molar fractions, namely, CO, H<sub>2</sub>, H, O, and OH, are negligible. However, the CO<sub>2</sub> has 3.5%, which is a substantial molar fraction as an emission. Besides, the CO and NO species as soot emission are most harmful products of the emission and have molar fractions of  $3.31 \times 10^{-8}$  and  $6.88 \times 10^{-4}$ , respectively. The effect of decision variables on these emissions investigated in the parametric study.

**Parametric study**

In this section, some input parameters are selected as major decision variables, and the effect of their variation on system performance is investigated. Accordingly, the pressure ratio, mass flow rate of injection from the top cycle and LP, IP, and HP pinch point temperature from the bottom cycle are selected as major decision variables. These parameters

**Table 10** Combustion products' molar fraction as a result of environmental assessment

Species	Molar Fraction
CO <sub>2</sub>	0.035
H <sub>2</sub> O	0.121
N <sub>2</sub>	0.774
O <sub>2</sub>	0.136
CO	3.31E-08
H <sub>2</sub>	5.10E-08
H	3.69E-10
O	1.20E-07
OH	1.83E-05
NO	6.88E-04

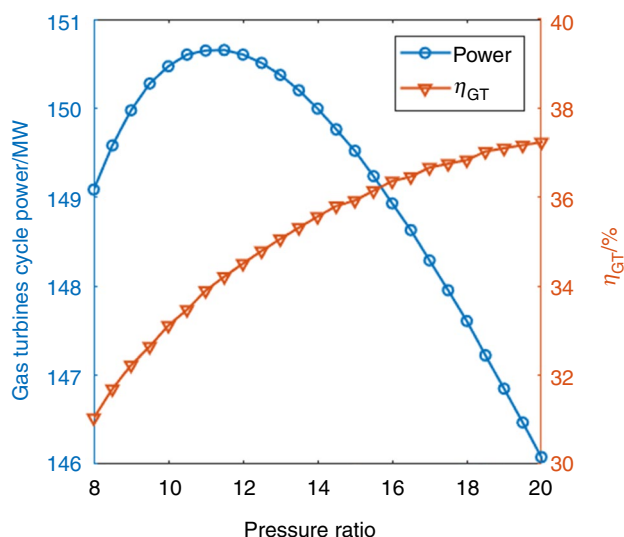


**Fig. 4** Effect of pressure ratio on the gas turbine cycle net power and efficiency

variation against the powers, efficiencies, exergy destruction investigated as energy and exergy analysis results. Besides, the effect of top cycle decision variables on CO and NO emission also presented as the environmental assessment result.

Figure 4 illustrates that increasing the pressure ratio of compressor and GT increases power consumption and production of both components, which have conflict effects on the gas turbine cycle power. As long as the pressure ratio is lower than 11, an increase in turbine outlet is more than that of compressor consumption, and after that compressor has

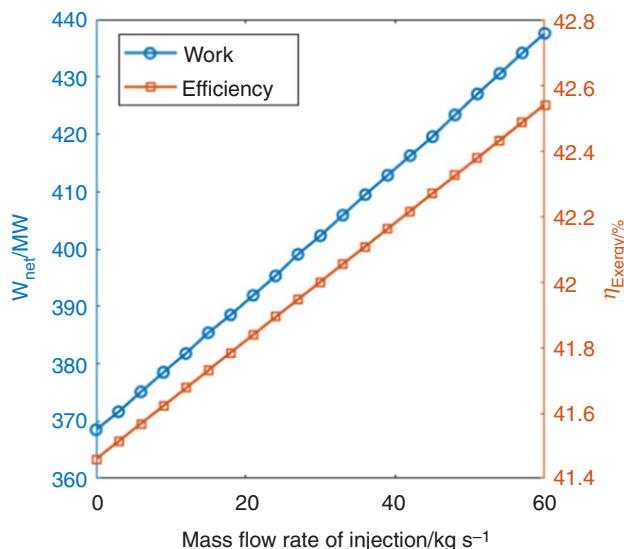


**Fig. 5** Effect of the mass flow rate of injection on total power and exergy efficiency

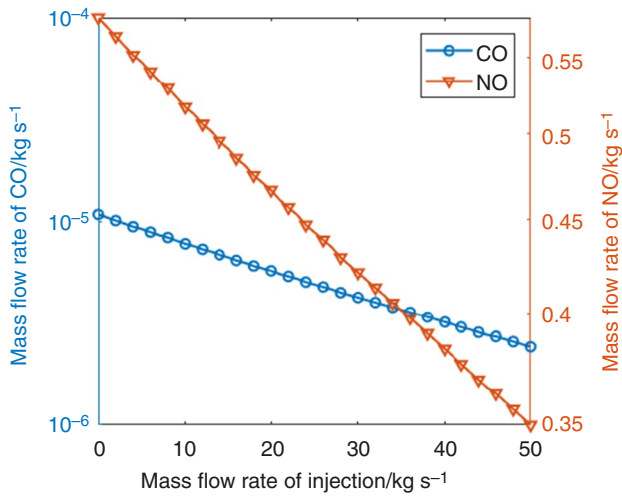


**Fig. 6** Effect of injection mass flow rate on the emissions mass flow rate

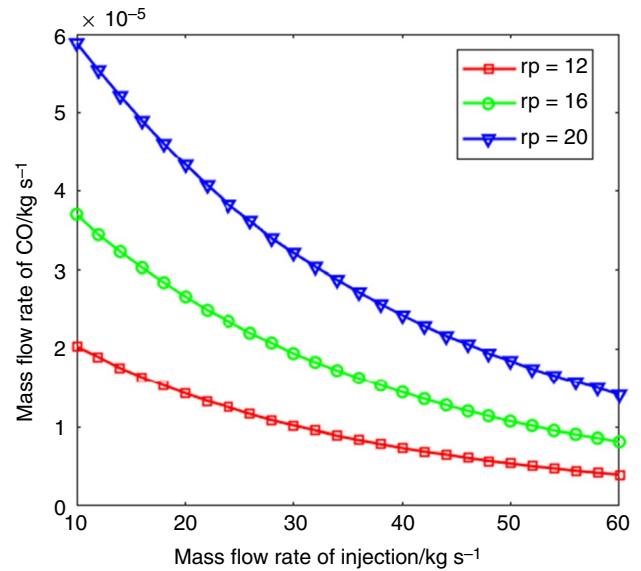


**Fig. 8** Effect of injection mass flow rate on the CO mass flow rate for various pressure ratio

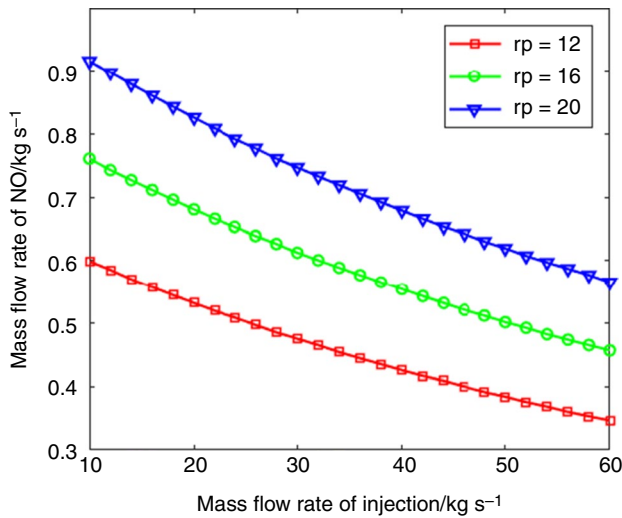


**Fig. 7** Effect of injection mass flow rate on NO mass flow rate for various pressure ratios

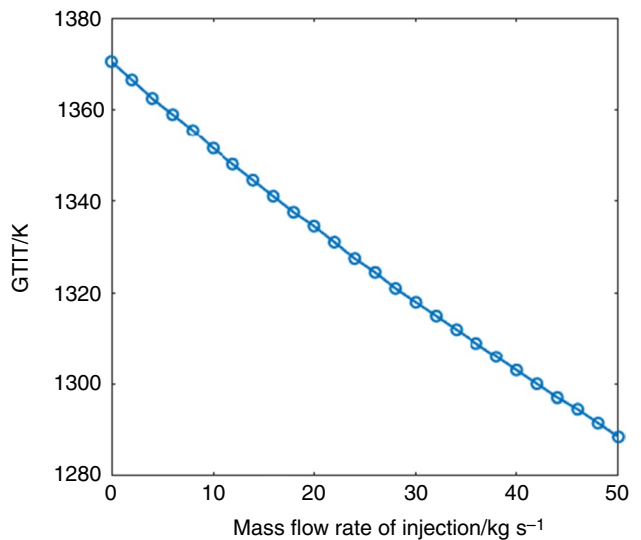


**Fig. 9** GTIT vs Mass flow rate of injection

a prevalent effect. Hence, the maximum gas turbine cycle power of 150.7 MW attained at pressure ratio of 11.

Besides, for constant combustion temperature, increasing pressure ratio raises compressor outlet temperature and reduces the amount of fuel needed to heat it up, so efficiency experiences a constant increase. Varying pressure ratios from 8 to 20, yields a variation in efficiency from 31.1% to 37.2% for the upstream gas turbine cycle.

Figure 5 illustrates the impact of the injected steams mass flow rate on net power and the overall exergy efficiency. Accordingly, increasing injection mass flow rate increases total flow rate of the exhaust and, therefore, generated power and efficiency. On average, each kilogram of injection leads

to 1 MW added production and an increase of 2.5% to the exergy efficiency.

Figure 6 shows that increasing the steam injection rate, results in combustion temperature reduction, and then reducing equilibrium constants and emissions. Increasing injection by 100 kilograms results in CO production being reduced to one-tenth of its original value, and NO emission is reduced from 0.57 to 0.4 kg. Note that these mass flow rates are for both gas turbine cycles in upstream, which has 1000 kg s<sup>-1</sup> mass flow rate.

**Fig. 10** Effect of **a** LP, **b** IP and **c** HP pinch point temperature on the overall exergy efficiency

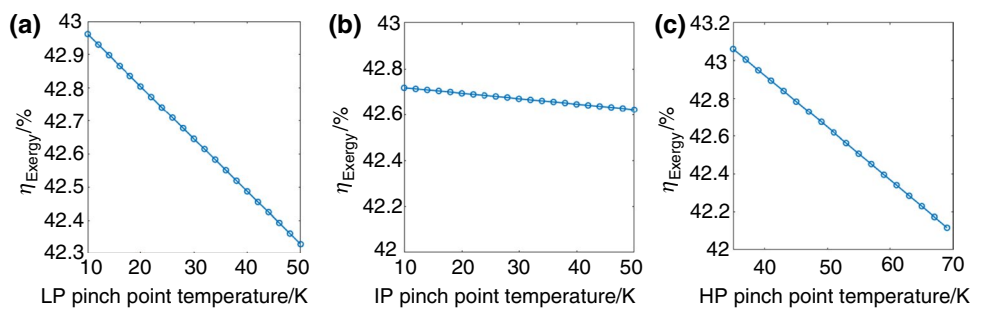
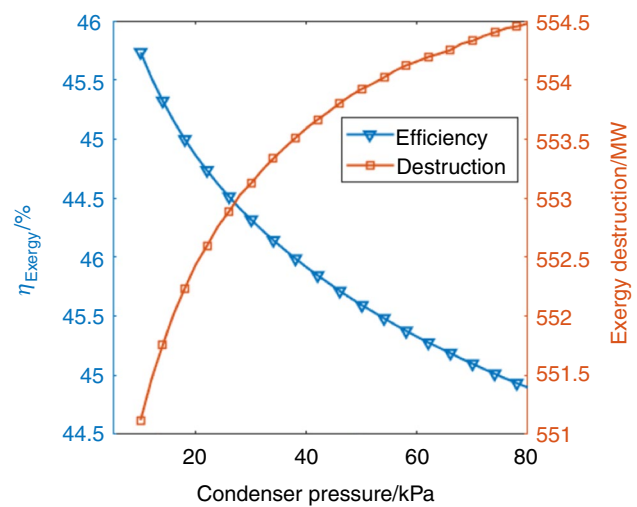


Figure 7 illustrates how injection mass flow rate impacts NO emission for various pressure ratios. Accordingly, increasing the mass flow rate decreases emissions, which was discussed in previous paragraph. In addition, three different pressure ratios investigated, which shows that lower pressure ratios for constant injection mass flow rate have lower emissions. Finally, it can be mentioned that the influence of the injection mass flow rate on emission control is more sensible on higher pressure ratios.

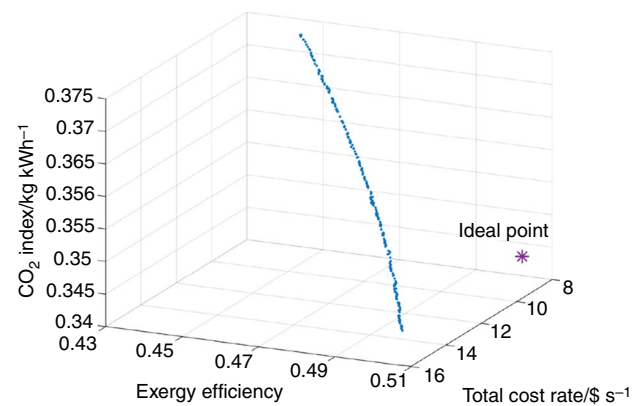
Figure 8 shows the effect of the injection mass flow rate on CO emission for various pressure ratios. Said figure shows a similar result to the previous figure. Accordingly, increasing the mass flow rate of injection from 10 to 60 kg s<sup>-1</sup> led the system to decreased CO emission mass flow rate from  $5.9 \times 10^{-5}$  to  $1.4 \times 10^{-5}$  for a pressure ratio of 20. Besides, decreasing the pressure ratio decreased the emission, and for higher pressure ratios, this reduction is more sensible.

Figure 9 illustrates the effect that injection mass flow rate has on flame temperature or gas turbine inlet temperature (GTIT). Accordingly, increasing the steam injection rate decreases combustion temperature, which is since the fuel energy is constant, and the combustion chamber inlet mass flow rate has been increased, so energy per mass, otherwise approximated as temperature, is reduced. In addition, for every 10 kg of steam injection, combustion temperature experiences a 20 K drop.

Figure 10a illustrates the effect of LP pinch point temperature on overall system exergy efficiency. Accordingly, increasing the LP pinch point temperature from 10 to 50 K leads the system to decrease the exergy efficiency from 42.96 to 42.33%. Figures 10b and c show the effect of IP and HP temperature on the exergy efficiency, which resulted similarly. Therefore, increasing the IP pinch point from 10 to 50 K results in an exergy efficiency reduction from 42.66% to 42.61%, and increasing the HP pinch point from 35 to 70 K leads the system to decrease the exergy efficiency from 43.08 to 42.12%. This reduction comes from the fact that increasing the pinch point stops the system from recovering more heat from the exhaust by the water and steam. Besides, the IP pinch point has a more sensible effect on the exergy efficiency due to the lower mass flow rate of this section.



**Fig. 11** Effect of condenser pressure on exergy efficiency and destruction



**Fig. 12** Pareto Frontier of exergy efficiency, total cost rate and CO<sub>2</sub> index multi-objective optimization

Figure 11 depicts the effect of condenser pressure on exergy efficiency and destruction. Accordingly, increasing the condenser pressure causes turbine work to be reduced since the area of the T-S diagram of the cycle is shrunken. Varying condenser pressure from 8 to 80 kPa results in

efficiency dropping from 45.7 to 45%, and exergy destruction decreased about 3 MW.

### Multi-objective optimization results

Figure 12 illustrates the Pareto Frontier of exergy efficiency, total cost rate, and carbon dioxide index as a result of genetic algorithm multi-objective optimization. As expected, the multi-objective optimization resulted in a curve as Pareto Frontier, which means that the two objectives have linear relation. In the proposed system, the CO<sub>2</sub> index changes inversely with exergy efficiency, which means increasing the exergy efficiency decreases the CO<sub>2</sub> index. Also, the Ideal Point of the Pareto Frontier, which is the point with maximum exergy efficiency and minimum total cost rate and CO<sub>2</sub> index, is represented in the graph in order to clarify the optimum points range. The values associated with the ideal

point are an exergy efficiency of 50.23%, a total cost rate of 8.04 \$/h, and a CO<sub>2</sub> index of 0.34 kg/kWh.

Figure 13 shows the scatter distribution of fuel stoichiometric ratio  $\lambda$ , steam injection flow rate, and gas turbine efficiency in all of which, Genetic Algorithm points are presented as well as the Pareto Frontier points. Using these figures, the optimum range of each decision variable can be found. Accordingly, Fig. 13a shows that the fuel stoichiometric ratio  $\lambda$  optimum value is distributed in a range of 0.026 to 0.04. Figure 13b illustrates that the optimum value for the steam injection flow rate is 46 kg s<sup>-1</sup>. Besides, Fig. 13(c) shows that the optimum range for gas turbine efficiency reaches a maximum possible value in the range of 89.5–90%.

Figure 14a depicts the scatter distribution of air compressor efficiency in which the optimum points of Pareto Frontier have a value of around 90%. Figure 14b shows a

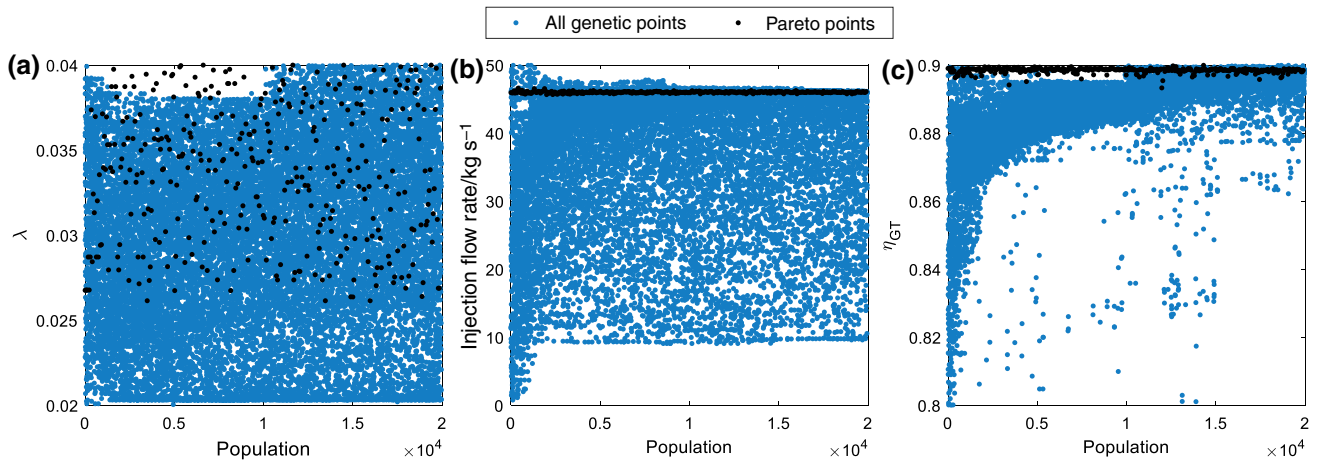


Fig. 13 Scatter distribution of **a** fuel stoichiometric ratio ( $\lambda$ ), **b** steam injection flow rate and **c** gas turbine efficiency

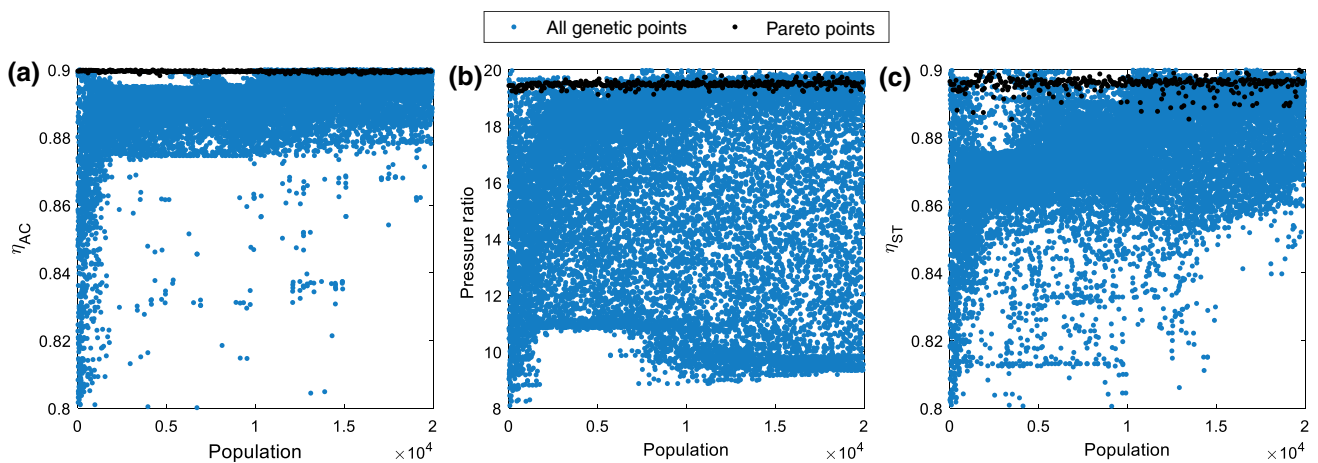
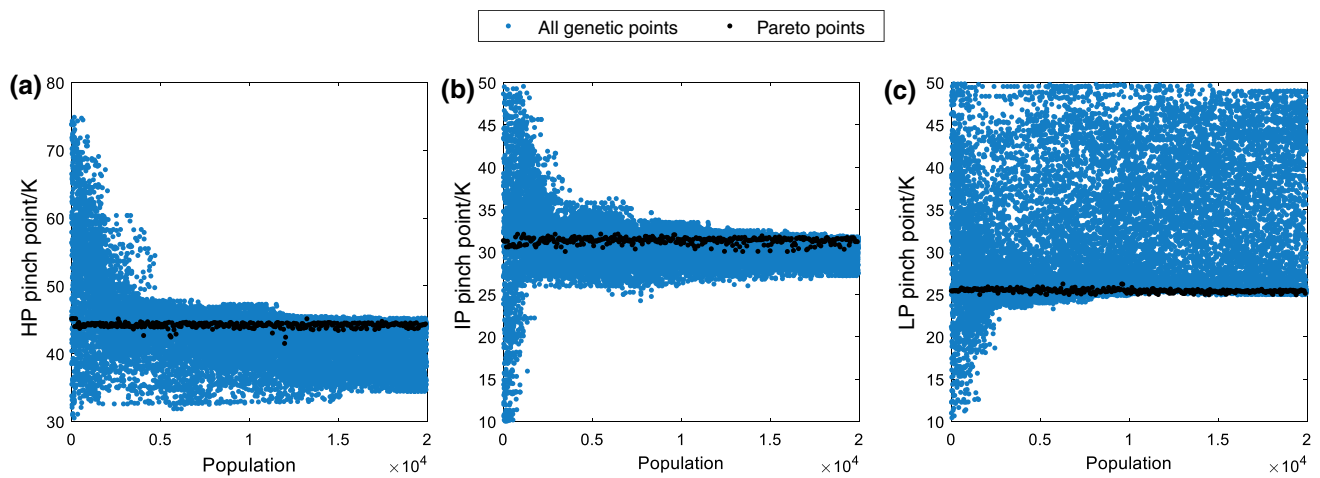
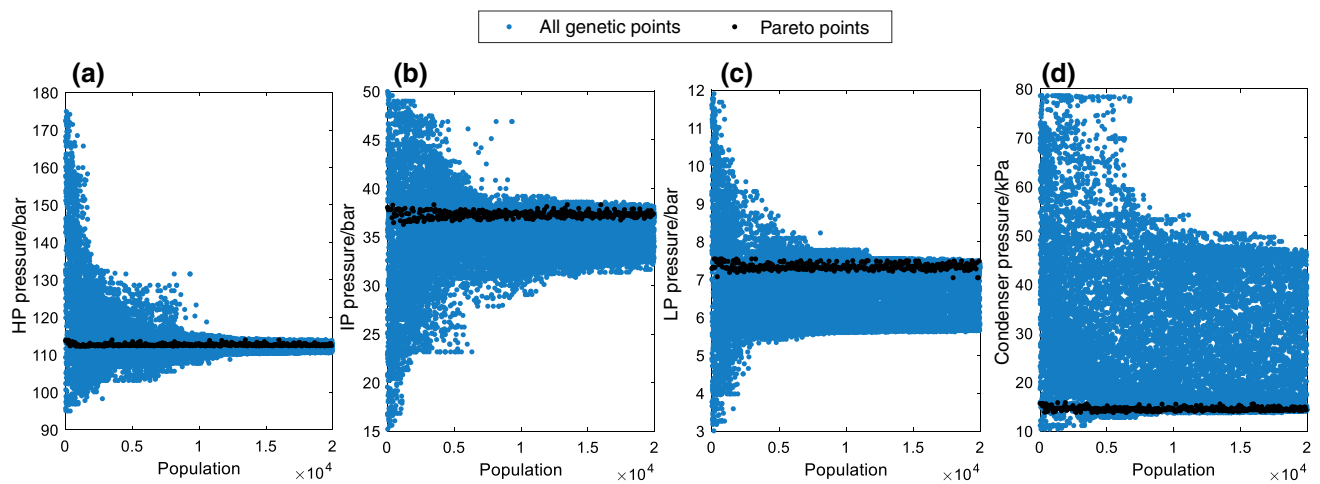


Fig. 14 Scatter distribution of **a** air compressor efficiency, **b** pressure ratio, **c** steam turbine efficiency



**Fig. 15** Scatter distribution of **a** HP pinch point, **b** IP pinch point, **c** LP pinch point temperature



**Fig. 16** Scatter distribution of **a** HP pressure, **b** IP pressure, **c** LP pressure and **d** condenser pressure

range between 19.1 and 19.8 for the optimum pressure ratio. Lastly, Fig. 14c presents the distribution of steam turbine efficiency for Pareto Points in which all points are located in a range of 88.5–90%.

Figure 15a presents the distribution of HP pinch point temperature values for the Pareto Frontier points, which resulted in a range of 41.5 to 45.1 K, HP pinch point to achieve an optimum result. Besides, Fig. 15b shows a range of 30 to 32 K for the IP pinch point, and Fig. 15c also shows a range of 25.1 K to 26.2 K for the optimum LP pinch point temperature.

The scatter distribution of HP pressure is shown in Fig. 16a from which the optimum range for HP pressure of HRSG is observed to be between 112 bar and 114 bar.

Figure 16b gives the optimum value between 36.5 and 38.3 bar for the IP pressure of HRSG. Figure 16c demonstrates an optimum range of 7–7.5 bar for the LP pressure. Finally, Fig. 16d shows that for an optimum result, the condenser pressure should be located in the range of 13 to 16 kPa.

## Conclusions

In this study, a novel combined cycle plant with steam injection is introduced in which the HRSG has a real case configuration with a triple-pressure HRSG to recover as much waste heat as possible from the exhaust. Besides,

the upstream cycle, which is a dual gas turbine cycle, has a steam injection at the combustion chamber to reduce hazardous emissions. The combustion process solved as accurately as possible in which the molar fraction of all types of emissions calculated utilizing the equilibrium constants. The energy, exergy, economic and environmental assessments are investigated, and the details of emission molar fractions are presented. Besides, a parametric study is done to analyze the effect of steam injection mass flow rate as well as the other main decision variables on system performance and emissions. Finally, a tri-objective optimization based on the Genetic Algorithm is done using MATLAB software in order to minimize emission and total cost rate, while maximizing the exergy efficiency simultaneously. As a result of the optimization, a 3D Pareto Frontier and scatter distribution of decision variables are shown to illustrate the range of optimum objective functions and decision variables. The conclusion and main results of this study are as follows:

- Referring to the exergy analysis, the condenser and the combustion chamber have the lowest exergy efficiency with values of 11.23% and 68.8%, respectively. Besides, the triple-pressure HRSG attained the exergy efficiency of 84.3%.
- According to economic analysis, the HRSG and condenser have the maximum purchase cost rate of 0.1673 and 0.1340 \$/s, respectively. In addition, the environmental costs calculated 6.24 \$/s, which is a substantial value compared against the total purchase cost rate of 0.5513 \$/s.
- The results of the environmental analysis show that in the study GTIT most emissions have molar fractions less than  $10^{-5}$  such as CO with molar fraction of  $3.31 \times 10^{-8}$ . However, the CO<sub>2</sub> and NO emissions had the molar fractions of 0.035 and  $6.88 \times 10^{-4}$ .
- The parametric studies pointed out that increasing the steam injection mass flow rate as well as decreasing the compressor pressure ratio reduces both CO and NO emissions significantly.
- The pinch point temperatures showed up a considerable effect on the overall exergy efficiency. However, among these pinch points, the LP pinch point temperature variation resulted in more changes in the overall exergy efficiency.
- The Pareto Frontier optimization result demonstrated the maximum achievable exergy efficiency of 50.23% in addition to the minimum total cost rate of 8.04 \$/h and CO<sub>2</sub> index of 0.34 kg/kWh as the Ideal Point.
- The scatter distributions indicate that the optimum value or range of decision variables in terms of exergy efficiency, total cost rate and CO<sub>2</sub> index are:  $0.026 < \lambda < 0.040$ ,  $\dot{m}_{\text{injection}} = 46 \text{ kg s}^{-1}$ ,  $0.895 < \eta_{\text{GT}} < 0.90$ ,  $\eta_{\text{AC}} = 0.90$ ,  $19.1 < \text{rp} < 19.8$ ,  $0.885 < \eta_{\text{ST}} < 0.90$ ,  $41.5 \text{ K} < T_{\text{pp,HP}} < 45.1 \text{ K}$ ,

$$30 \text{ K} < T_{\text{pp,IP}} < 32 \text{ K}, 25.1 \text{ K} < T_{\text{pp,LP}} < 26.2 \text{ K}, \\ 112 \text{ bar} < P_{\text{HP}} < 114 \text{ bar}, 36.5 \text{ bar} < P_{\text{IP}} < 38.3 \text{ bar}, \\ 7 \text{ bar} < P_{\text{LP}} < 7.5 \text{ bar}, 13 \text{ kPa} < P_{\text{Cond}} < 16 \text{ kPa}.$$

## References

1. McNamara MC, Niaraki-Asli AE, Guo J, Okuzono J, Montazami R, Hashemi NN. Enhancing the conductivity of cell-laden alginate microfibers with aqueous graphene for neural applications. *Front Mater*. 2020. <https://doi.org/10.3389/fmats.2020.00061>.
2. Mousavi SA, Zarchi RA, Astaraei FR, Ghasempour R, Khaninezhad FM. Decision-making between renewable energy configurations and grid extension to simultaneously supply electrical power and fresh water in remote villages for five different climate zones. *J Clean Prod*. 2021;279:123617.
3. Iman F, Amirmohammad B, Ehsan G, Pouria A, Ahmad A (2021) Comparative double and integer optimization of low-grade heat recovery from PEM fuel cells employing an organic Rankine cycle with zeotropic mixtures. *Energy Convers Manag* 228:113695
4. Kiani M, Houshfar E, Asli AEN, Ashjaee M. Combustion of syngas in intersecting burners using the interferometry method. *Energy & Fuels*. 2017;31(9):10121–32.
5. Ahmadi P, Dincer I. Exergoenvironmental analysis and optimization of a cogeneration plant system using Multimodal Genetic Algorithm (MGA). *Energy*. 2010;35(12):5161–72.
6. Lozano MA, Valero A. Theory of the exergetic cost. *Energy*. 1993;18:939.
7. Lazzaretto A, Tsatsaronis G. PECO: a systematic and general methodology for calculating efficiencies and costs in thermal systems. *Energy*. 2006;31(8–9):1257–89.
8. Namin AS, Rostamzadeh H, Nourani P. Thermodynamic and thermoeconomic analysis of three cascade power plants coupled with RO desalination unit, driven by a salinity-gradient solar pond. *Therm Sci Eng Prog*. 2020;18:100562.
9. Mohagheghi M, Shayegan J. Thermodynamic optimization of design variables and heat exchangers layout in HRSGs for CCGT, using genetic algorithm. *Appl Therm Eng*. 2009;29(2):290–9.
10. Bracco S, Siri S. Exergetic optimization of single level combined gas-steam power plants considering different objective functions. *Energy*. 2010;35(12):5365–73.
11. Woudstra N, Woudstra T, Pirone A, van der Stelt T. Thermodynamic evaluation of combined cycle plants. *Energy Convers Manag*. 2010;51(5):1099–110.
12. Franco A, Casarosa C. Thermoeconomic evaluation of the feasibility of highly efficient combined cycle power plants. *Energy*. 2004;29(12):1963–82.
13. Valdés M, Rapún JL. Optimization of heat recovery steam generators for combined cycle gas turbine power plants. *Appl Therm Eng*. 2001;21(11):1149–59.
14. Bassily AM. Modeling, numerical optimization, and irreversibility reduction of a dual-pressure reheat combined-cycle. *Appl Energy*. 2005;81(2):127–51.
15. Bassily AM. Modeling, numerical optimization, and irreversibility reduction of a triple-pressure reheat combined cycle. *Energy*. 2007;32(5):778–94.
16. Valdés M, Durán MD, Rovira A. Thermoeconomic optimization of combined cycle gas turbine power plants using genetic algorithms. *Appl Therm Eng*. 2003;23(17):2169–82.
17. Casarosa C, Donatini F, Franco A. Thermoeconomic optimization of heat recovery steam generators operating parameters for combined plants. *Energy*. 2004;29(3):389–414.



18. Tyagi KP, Khan MN. Effect of gas turbine exhaust temperature, stack temperature and ambient temperature on overall efficiency of combine cycle power plant. *Int J Eng Technol.* 2010;2(6):427–9.
19. Boonnasa S, Namprakai P, Muangnapoh T. Performance improvement of the combined cycle power plant by intake air cooling using an absorption chiller. *Energy.* 2006;31(12):2036–46.
20. Kwak HY, Kim DJ, Jeon JS. Exergetic and thermoeconomic analyses of power plants. *Energy.* 2003;28(4):343–60.
21. Fiaschi D, Manfrida G. Exergy analysis of the semi-closed gas turbine combined cycle (SCGT/CC). *Energy Convers Manag.* 1998;39(16):1643–52.
22. Cihan A, Hacıhafızoğlu O, Kahveci K. Energy-exergy analysis and modernization suggestions for a combined-cycle power plant. *Int J Energy Res.* 2006;30(2):115–26.
23. Kilani N, Khir T, Ben Brahim A. Performance analysis of two combined cycle power plants with different steam injection system design. *Int J Hydrogen Energy.* 2017;42(17):12856–64.
24. Mokhtari H, Ahmadisedigh H, Ameri M. The optimal design and 4E analysis of double pressure HRSG utilizing steam injection for Damavand power plant. *Energy.* 2017;118:399–413.
25. Athari H, Soltani S, Rosen MA, Gavifekr MK, Morosuk T. Exergoeconomic study of gas turbine steam injection and combined power cycles using fog inlet cooling and biomass fuel. *Renew. Energy.* 2016;96:715–26.
26. *Internal Combustion Engines: Applied Thermosciences*, 3rd Edition. Wiley.
27. Bejan A, George Tsatsaronis G, Moran MJ. *Thermal design and optimization.* Hoboken: Wiley; 1996.
28. Fakhari I, Behzadi A, Gholamian E, Ahmadi P, Arabkoohsar A. Design and tri-objective optimization of a hybrid efficient energy system for tri-generation, based on PEM fuel cell and MED using syngas as a fuel. *J Clean Prod.* 2020. <https://doi.org/10.1016/j.jclepro.2020.125205>.
29. Dincer I, Rosen MA, Ahmadi P. *Optimization of energy systems.* New York: Wiley; 2017.
30. Shams Ghoreishi SM, et al. Analysis, economical and technical enhancement of an organic Rankine cycle recovering waste heat from an exhaust gas stream. *Energy Sci Eng.* 2019;7(1):230–54.
31. Noroozian A, Mohammadi A, Bidi M, Ahmadi MH. Energy, exergy and economic analyses of a novel system to recover waste heat and water in steam power plants. *Energy Convers Manag.* 2017;144:351–60.
32. Mohammadi A, Ashouri M, Ahmadi MH, Bidi M, Sadeghzadeh M, Ming T. Thermoeconomic analysis and multiobjective optimization of a combined gas turbine, steam, and organic Rankine cycle. *Energy Sci Eng.* 2018;6(5):506–22.
33. Ahmadi P, Dincer I, Rosen MA. Exergy, exergoeconomic and environmental analyses and evolutionary algorithm based multi-objective optimization of combined cycle power plants. *Energy.* 2011;36(10):5886–98.
34. Ferguson CR, Kirkpatrick A. *Internal combustion engines: applied thermosciences.* Hoboken: Wiley; 2015.
35. Ameri M, Ahmadi P, Khanmohammadi S. Exergy analysis of a 420 MW combined cycle power plant. *Int J Energy Res.* 2008;32(2):175–83.

**Publisher's Note** Springer Nature remains neutral with regard to jurisdictional claims in published maps and institutional affiliations.